Performances of domiciliary ventilators compared by using a parametric procedure

Emeline Fresnel, Jean-Francois Muir, Christophe Letellier

Fresnel *et al. EPJ Nonlinear Biomedical Physics* (2016) 4:6
DOI 10.1140/epjnbp/s40366-016-0033-9

EPJ Nonlinear Biomedical Physics
a SpringerOpen Journal

RESEARCH Open Access

Performances of domiciliary ventilators compared by using a parametric procedure

Emeline Fresnel[1,2,3*], Jean-François Muir[3] and Christophe Letellier[1,2]

*Correspondence:
emeline.fresnel@coria.fr
[1]CORIA UMR 6614 — Normandie Université, CNRS-Université et INSA de Rouen, Campus Universitaire du Madrillet, F-76800, Saint-Etienne du Rouvray, France
[2]ADIR Association, Hôpital de Bois-Guillaume, F-76031, Rouen, France
Full list of author information is available at the end of the article

Abstract

Background: Noninvasive mechanical ventilation is sufficiently widely used to motivate bench studies for evaluating and comparing performances of the domiciliary ventilators. In most (if not in all) of the previous studies, ventilators were tested in a single (or a very few) conditions, chosen to avoid asynchrony events. Such a practice does not reflect how the ventilator is able to answer the demand from a large cohort of patients with their inherent inter-patient variability. We thus developed a new procedure according which each ventilator was tested with more than 1200 "simulated" patients.

Methods: Three lung mechanics (obstructive, restrictive and normal) were simulated using a mechanical lung (ASL 5000) driven by a realistic muscular pressure. 420 different dynamics for each of these three lung mechanics were considered by varying the breathing frequency and the mouth occlusion pressure. For each of the nine ventilators tested, five different parameter settings were investigated. The results are synthesized in colored maps where each color represents the ventilator (in)ability to synchronize with a given muscular pressure dynamics. A synchronizability ε is then computed for each map.

Results: The lung model, the breathing frequency and the mouth occlusion pressure strongly affect the synchronizability of ventilators. The Vivo 50 (Breas) and the SomnoVENT autoST (Weinmann) are well synchronized with the restrictive model ($\overline{\varepsilon} = 86$ and 78 %, respectively), whereas the Elisée 150 (ResMed), the BiPAP A40 and the Trilogy 100 (Philips Respironics) better fit with an obstructive lung mechanics ($\overline{\varepsilon} = 87$, 86 and 86 %, respectively). Triggering and pressurization performances of the nine ventilators present heterogeneities due to their different settings and operating strategies.

Conclusion: Performances of domiciliary ventilators strongly depend not only on the breathing dynamics but also on the ventilator strategy. One given ventilator may be more adequate than another one for a given patient.

Keywords: Noninvasive ventilation, Lung model, Patient-ventilator interaction, Ventilator performances

Background

The use of noninvasive ventilation (NIV) strongly increased during the last twenty years, and became a common technique for managing acute and chronic respiratory failures. In response to a growing market, manufacturers propose yearly (if not more often) new ventilators with an increasing number of ventilatory modes and settings. Our objective

is to help the physicians to improve the synchronization between the ventilator pressure cycles and patient breathing cycles, a key feature to optimize comfort and reduce the work of breathing [1]. The number of parameters available in a modern ventilator is indeed significantly greater than in those produced one or two decades ago. Unfortunately, the terminology used to designate these ventilator settings remains not unified and the same abbreviation can sometimes correspond to different quantities, as clearly pointed out long time ago [2]. Such disparities make a comparison between the different ventilators difficult to establish.

In spite of this, several bench studies were published for evaluating and comparing the performances of these devices. However, there is no standardized protocol for bench studies [3] and, for instance, some parameters used to set the lung model or the ventilators are not systematically reported: it is therefore not possible to reproduce most of these studies. Moreover, although bench studies seem to be the most reliable and efficient way to compare mechanical ventilators [4–7], it is difficult to know whether the devices were actually tested in equivalent working conditions, and different studies can sometimes lead to conflicting results. Each parameter used to set the lung model and the ventilator to perform bench tests should therefore be explicitly specified and translated in the same units (by using specific external measurements) for each device to allow rigorous comparisons. Such a step is required to develop a procedure to compare mechanical ventilators for helping physicians to more objectively select an adequate ventilator for their patient respiratory profile since performances are known to depend on it [4].

Among available ventilatory parameters, the sensitivity to patient inspiratory effort for triggering the pressure rise (here designated as the pressure rise triggering sensitivity or the high pressure triggering sensitivity) appears to be the most significant setting in pressure support ventilation since it directly affects the synchronization between the pressure cycle and the respiratory demand [8]. A lack of synchronization such as the presence of non-triggered cycles reduces patient comfort and increases the work of breathing [1, 9]. It is thus relevant to assess the abilities of ventilators to correctly synchronize their pressure cycles with patient inspiratory demand. Assessing triggering sensitivity performances is a non trivial task [3, 10, 11], mainly because different algorithms are used by the manufacturers to detect inspiratory efforts. It is therefore difficult to propose a standard measure to evaluate their performances. We are not yet able to propose an external measure allowing to compare objectively the sensitivity of the pressure rise triggering rather than counting the different types of asynchrony events. Pressure rise duration is also a key parameter which affects patient's inspiratory work load [12], and must be taken into account for optimizing patient-ventilator interactions. A key parameter is the trigger to switch from the high to the low pressure delivered by the ventilator (here designated as the low pressure trigger or the pressure release trigger and often designated elsewhere as the "cycling"). These last two parameters are easier to compare because they are more or less based on similar algorithms and can be easily evaluated by the pressure rise duration and the percentage of the maximum airflow reached during the running cycle, respectively.

In the present work, we developed a procedure to test the abilities of domiciliary ventilators to correctly synchronize the pressure cycles they deliver with patient breathing cycles in various conditions. We developed our procedure in trying to overcome some of the weaknesses pointed out in the critical analysis of bench studies evaluating devices

for noninvasive ventilation recently published [3]. We therefore focused our attention in elaborating a protocol providing reliable and reproducible results. First, we based our tests by simulating patient breathing cycles with the help of a realistic muscular pressure as developed in [13] for driving our mechanical lung (an ASL 5000, Ingmar Medical, Pittsburgh, USA). In order to avoid the situation where two different ventilators are tested in two different operating conditions, each ventilator was parametrized in a systematic way and was tested with a large set of lung dynamics; from our point of view, this is a very key point since testing a ventilator with a single lung dynamics can lead to two opposite biased situations; i) the lung dynamics was an example chosen because the ventilator manages it in an optimal way and ii) the lung dynamics is unfortunately one of those the ventilator is not able to synchronize with. In the former case, the performances of the ventilator are overestimated while they are underestimated in the latter case. In both cases, the ventilator is incorrectly evaluated. We therefore introduce a parametric test, that is, each ventilator is tested with three types of lung mechanics (restrictive, obstructive and normal) whose dynamics is varied in a wide range to simulate a large cohort of patients.

Methods

In the subsequent part of this paper, a time at which an event occurs is designated by T_{event}, the time interval (the duration) during which a process happens by τ_{process} and the delay with which an event occurs compared to the expected time by δ_{event}. This notation will avoid to mistake times, durations and delays.

Lung model and simulated inspiratory effort

Among the different types of mechanical lungs available, we used a microprocessor-controlled piston, the ASL 5000. The choice for this device results from the fact that this is an active and flexible mechanical lung that has become extensively used for testing performances of domiciliary ventilators [14–19]. It consists in a computer controlled piston-cylinder unit whose mechanics can be adjusted by realistic parameters such as the resistance of the airways and the lung compliance, and whose dynamics can be varied according to parameters as the breathing frequency and the amplitude of the muscular pressure. In all cases, ventilators were connected to the mechanical lung *via* a single tube with intentional leaks. If not compatible with the ventilator, this interface was substituted by a single tube with an expiratory valve. Pressure, airflow and muscular pressure signals were measured with the ASL 5000 software at 512 Hz and stored for subsequent analysis. The data were then processed with the help of a code written by us and based on the definition of asynchrony events as detailed below.

The inter-patient variability clinically observed can therefore be easily simulated. There is not yet a consensus for designing the evolution of the muscular pressure for driving an ASL [3] and all parameter values required to reproduce it are very rarely fully reported, with the exception of Chatburn's studies [20]. Most often a semi-sinusoidal muscle pressure — as predefined in the ASL 5000 — is used. Based on the (rare) physiological data available, we thus developed a more realistic evolution of the muscular pressure (Fig. 1) [13].

The respiratory muscle pressure was simulated by using two exponential functions, one for inspiration and one for expiration (see [13] for details). The whole breathing cycle

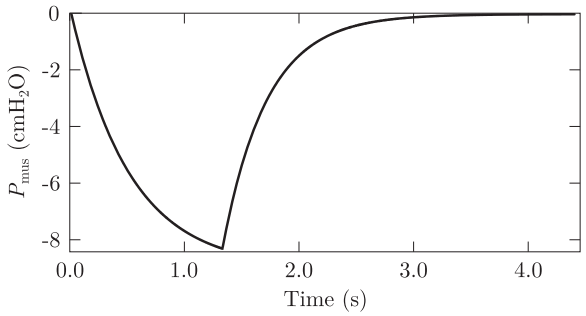

Fig. 1 Realistic muscular pressure P_{mus}. Muscular pressure model used for driving the ASL 5000 as developed by Fresnel et al. [13]

thus simulated only depends on two clinical parameters that are i) the breathing frequency f_b and ii) the mouth occlusion pressure $P_{0.1}$ at 0.1s representing the stiffness of the inspiratory effort.

From these two parameters and the formula governing the exponential evolution of the muscular pressure, the maximum amplitude P_{max} and the duration τ_{ins} of the contraction (corresponding to the inspiratory phase) and the duration τ_{exp} of the relaxation (corresponding to the expiratory phase) are automatically computed by using [13]

$$\frac{\tau_{ins}}{\tau_{tot}} = 0.0125 f_b + 0.125 \quad \text{where} \quad \tau_{tot} = \frac{60}{f_b}. \tag{1}$$

According to clinical studies [21–24], most of patho-physiological cases are considered when $P_{0.1}$ is varied from 0.5 to 10 cmH$_2$O (with an increment equal to 0.5 cmH$_2$O). Combined with the breathing frequency f_b which is varied from 10 to 30 cycles per minute (cpm) with an increment equal to 1 cpm, it allows to model 420 different ventilatory dynamics, each pair $(f_b, P_{0.1})$ corresponding to a given lung mechanics (or a "simulated" patient in a clinical equivalent). The maximum amplitude [13]

$$P_{max} = \frac{P_{0.1}}{1 - e^{\frac{-0.1(f_b + 4 \cdot P_{0.1})}{10}}} \tag{2}$$

of the muscular pressure is thus between 2 and 25 cmH$_2$O, in agreement with the recommendations proposed by Olivieri el al., allowing to simulate weak (2 cmH$_2$O), normal (8 cmH$_2$O), high (15 cmH$_2$O) and strenuous (25 cmH$_2$O) inspiratory efforts [3].

Three lung mechanics were chosen to simulate normal, obstructive and restrictive disorders in the lung. The corresponding values of the airway resistance and the lung compliance (Table 1) were chosen within the range commonly found in bench studies and are close to the values proposed by Olivieri et al. to model severe obstruction and restriction, respectively [3]. Each ventilator is therefore tested with a total of 1260 different ventilatory dynamics. In each case, 50 breathing cycles were simulated.

Table 1 Values of the airway resistance R and the lung compliance C used to simulate the three lung mechanics

	Normal	Restrictive	Obstructive
R (cmH$_2$O.s/l)	5	5	25
C (ml/cmH$_2$O)	50	20	50

Ventilator modes and the different types of cycles

In this work, we choose to focus on the pressure support mode since it is available in any device from the market and is the most often used mode at home [25]. This ventilation mode consists in a partial support provided by a positive pressure cycle ideally synchronized with patient's breathing cycles. It offers numerous advantages among which the fact that it is often easily accepted by the patients [26]. This mode is labeled in various ways in the different ventilators we tested. Thus, it is mode "S" in the Trilogy 100 (Philips Respironics), the BiPAP A40 (Philips Respironics), the S9 VPAP ST (ResMed), the Stellar 100 (ResMed), and the SOMNOvent autoST (Weinmann). It is mode "PS" in the Elisée 150 (ResMed), and mode "PSV" in the Vivo 50 (Breas), the Monnal T50 (Air Liquide Medical Systems) and the Smartair ST (Covidien). Typically, this mode is based on two phases, one with a high pressure during the inspiration and one with a low pressure during the expiration. One pressure cycle was therefore associated with a detection of the inspiratory effort that triggers the pressure rise from the low to the high pressure level, and a detection of the relaxation of the inspiratory demand for triggering the pressure release from the high to the low pressure level. This mode gives priority to the synchronization between the patient breathing cycles (here simulated by the mechanical lung) and the pressure cycles delivered by the ventilator. It is therefore necessary to introduce a terminology that clearly distinguishes the patient breathing cycles from the ventilator pressure cycles.

The main characteristics of the ventilator pressure cycles are the delivery of a high pressure P_{h} (corresponding to the so-called IPAP for "inspiratory positive airway pressure") and a low pressure P_{l} (corresponding to the so-called EPAP for "expiratory positive airway pressure" or PEEP for "positive end-expiratory pressure"). The point that motivated this new terminology is that the pressure cycle delivered by the ventilator is not always synchronized with the patient breathing cycle: the high pressure P_{h} is therefore not necessarily delivered during patient's inspiration, hence turning the term "positive inspiratory pressure" ambiguous [27].

To trigger the two pressure switches occurring during a pressure cycle, the ventilators use an algorithm interpreting measurements of the airflow Q_{v} and the pressure P_{v} within the ventilation circuit. First, there is a switch ensuring a transition from the low pressure to the high pressure level at time T_{h} induced by the detection of patient's inspiratory effort; such a switch is commonly triggered from the airflow Q_{v}, using a threshold or a variation of that airflow within an interval of a few milliseconds. Second, there is a switch ensuring the pressure release to the low level at time T_{l}, also triggered by a condition on the airflow commonly expressed as a fraction of the maximum airflow $Q_{\mathrm{v,\,max}}$ achieved during the running cycle (Fig. 2). These switches depend on the here-called high pressure triggering sensitivity η_h (or the pressure rise triggering sensitivity) and on the low pressure triggering sensitivity η_l (or the pressure release triggering sensitivity) regardless of the ventilator strategy. We prefer to speak in terms of triggering because it corresponds explicitly to the processes actually used by the ventilator to drive the pressure cycles it delivers. During mechanical ventilation, the breathing cycle combines with the pressure cycle to provide the "ventilatory cycle" which is the one actually investigated from the measurements of the airflow and the pressure in the ventilatory circuit. When the pressure cycle is synchronized with the breathing cycle, the ventilatory cycle is also synchronized with the two "primary" cycles. Typically when there are asynchrony

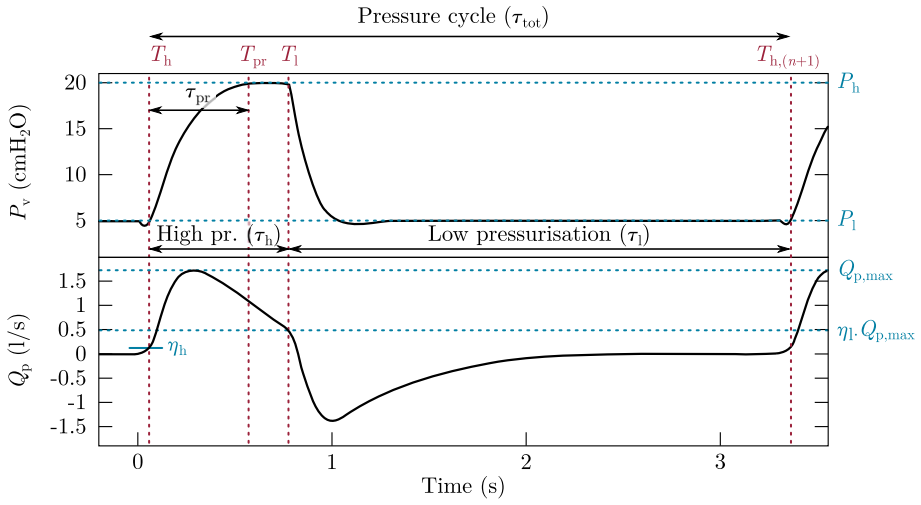

Fig. 2 Ventilatory curves from the mechanical lung. The pressure P_v and the mechanical lung airflow Q_p measured in the mechanical lung (or Q_v in the ventilatory circuit in clinical situations) connected to a ventilator in pressure support mode are plotted. P_h is the high pressure, P_l the low pressure, $Q_{p,max}$ the maximum airflow reached in the running cycle, η_h corresponds to the high pressure triggering sensitivity, η_l to the low pressure triggering sensitivity and τ_{pr} to the pressure rise duration

events, by definition, the ventilatory cycle is not synchronized with the breathing cycle, thus justifying to distinguish these three different cycles.

Once the pressure rise is triggered, the transition between the low and high pressure levels, corresponding to the level of ventilatory support $\Delta P = P_h - P_l$, can be reached more or less rapidly. The duration of this "pressure rise" is computed from time T_h at which the pressure rise is triggered by the ventilator and time T_{pr} at which the high pressure P_h is reached. This duration is expressed as

$$\tau_{pr} = T_{pr} - T_h \tag{3}$$

where τ_{pr} designates the duration of the pressure rise whereas T_{pr} designates the time at which the high pressure is reached. In order to simplify comparisons, this term τ_{pr} will be used to express the pressure rise duration computed from the measured ventilatory pressure, even when the parameter is not expressed as a duration in the ventilator.

The ventilatory cycle can therefore be characterized by the four durations as follows (Fig. 2). First, there is the high pressure phase duration $\tau_h = T_l - T_h$, which includes the pressure rise duration $\tau_{pr} = T_{pr} - T_h$. Then there is the low pressure phase duration $\tau_l = T_{h,(n+1)} - T_l$. The total cycle duration $\tau_{tot} = T_{h,(n+1)} - T_h$ obviously corresponds to $\tau_h + \tau_l$. In these previous definitions, T_h ($T_{h,(n+1)}$) is the time at which the nth ($n + 1$th) high pressure rise is triggered.

Our objective is to assess the performances of ventilators that are connected to three lung models as previously defined. We investigated these performances in varying two of the most important parameters which influence the synchronization between patient's breathing cycles and ventilator pressure cycles. We thus varied the high pressure triggering sensitivity η_h [8] and, the pressure rise duration τ_{pr} [28]. Although it is known that the low pressure P_l [29] and the pressure support level $\Delta P = P_h - P_l$ [9, 30] are particularly crucial to avoid deleterious asynchrony events such as non-triggered cycles or double-triggered cycles, Costa et al. also focused on η_h and τ_{pr} [19]. Since each parameter

settings (five for each ventilator) is tested for a cohort of 1260 simulated lung dynamics, we limited the number of parameter values: the low pressure P_l was therefore set to 5 $\mathrm{cmH_2O}$, and the high pressure P_h to 20 $\mathrm{cmH_2O}$, corresponding to a pressure support of 15 $\mathrm{cmH_2O}$. According to Olivieri et al. [3], this low pressure is most common value, and the retained high pressure is the largest used in test bench studies.

In practice, each ventilator has its own process for triggering the pressure rise and may work in a very specific way. Some ventilators, such as the Vivo 50 for instance, use triggering conditions which differ rather significantly from those used by the other devices. Consequently, it is not always possible to have the same operating conditions for all the ventilators involved in a comparative test. We investigated triggering performances for three sensitivity values η_h corresponding to the highest, the median and the lowest sensitivity in the range proposed in each ventilator (the highest sensitivity being associated with the smallest inspiratory effort provided by the lung model to trigger the pressure rise). We then choose to assess the sensitivity of the high pressure triggering by measuring the mechanical lung airflow Q_p and the muscular pressure P_mus when the pressure rise starts, thus allowing direct comparisons.

The low pressure triggering sensitivity η_l is more consensual among manufacturers. It is commonly defined as a fraction Q_l of the maximum airflow $Q_{\mathrm{p,\,max}}$ reached during the running cycle. Depending on the ventilator, there are two ways to define this threshold Q_l which may either correspond to $Q_\mathrm{l} = \eta_\mathrm{l}\, Q_{\mathrm{p,\,max}}$ or to $Q_\mathrm{l} = (1 - \eta_\mathrm{l})\, Q_{\mathrm{p,\,max}}$. This is here another source of confusion for clinicians. We will use the first way for reporting the values we selected for η_l. In our protocol, in order to limit the number of parameters to vary, η_l is set to a given value for each lung mechanics tested. We did our best to set the low pressure triggering sensitivity η_l to 25 % for the restrictive mechanics, 30 % for the normal model and 75 % for the obstructive model to reduce expiratory flow limitation which affects these latter patients [31]. In fact, it was shown that recent bilevel ventilators tend to trigger prematurely the pressure release when connected to normal lung mechanics, a tendency exacerbated with a restrictive lung. With our obstructive lung, this release is delayed, a feature which is aggravated in the presence of air leaks [32].

The pressure can rise according to a linear or an exponential function. Most often, there is no information concerning the exact duration of the pressure rise, and it is difficult to know which value is considered by the ventilator. Consequently, in order to allow objective comparison, as we did for the high pressure triggering sensitivity, the pressure rise duration was investigated for the shortest, median and longest settings available in each ventilator. The effective duration was then measured as the duration between time T_h at which the high pressure rise is triggered and the time $T_{0.95P}$ at which the pressure reaches 95 % of the maximum pressure observed during the running cycle.

In modern ventilators, two additional parameters are available: they are the minimal ($\tau_{\mathrm{h,\,min}}$) and maximal ($\tau_{h,\mathrm{max}}$) durations for which the high pressure is delivered. These two settings may override the pressure release, that is, the ventilator ability to detect the end of patient's inspiratory effort. In the present work, we therefore choose $\tau_{\mathrm{h,\,min}}$ ($\tau_{\mathrm{h,\,max}}$) equals to the minimum (maximum) value proposed by the ventilator to avoid any influence of these parameters on our results. Depending on the possibilities offered by the ventilator, we set off the backup frequency or set it at the minimum value. Selected parameter values for the tested ventilators are reported in Table 2.

Table 2 Minimum, median and maximum values for three parameters which were varied in the domiciliary ventilators tested in our protocol

	High pressure triggering sensitivity η_h			Pressure rise duration τ_{pr}			Low pressure triggering sensitivity η_l		
	Maximum	Median	Minimum	Minimum	Median	Maximum	Restrictive	Normal	Obstructive
BiPAP A40†	1 l/min	5 l/min	9 l/min	1	3	6	25 %	30 %	75 %
Elisée 150‡	1	3	5	1	2	4	25 %	30 %	75 %
Monnal T50◇	0.5 l/min	5 l/min	10 l/min	1	2	4	25 %	30 %	75 %
S9 VPAP ST‡	Very high	Medium	Very low	Min	500 ms	900 ms	Very low	Low	Very high
Smartair ST*	1	3	5	1	2	4	–75 %	–70 %	–25 %
SOMNOvent autoST⋆	–1	Std	1	Std	Soft	ESoft	—	—	—
Stellar 100‡	Very high	Medium	Very low	MIN	500 ms	900 ms	Very low	Low	Very high
Trilogy 100†	1 l/min	5 l/min	9 l/min	1	3	6	25 %	30 %	75 %
Vivo 50♮	1	5	9	1	5	9	7	7	3

†: Philips Respironics
‡: ResMed
◇: Air Liquide Medical Systems
*: Covidien
⋆: Weinmann
♮: Breas

Dynamics of the lung model-ventilator system

In our simulations, the muscular pressure curve which drives the mechanical lung is noise free and the inspiratory effort initiation is therefore known precisely: the corresponding time is designated by T_0. Since the high pressure rise starts at time T_h, the high pressure triggering delay δ_h thus corresponds to

$$\delta_\mathrm{h} = T_\mathrm{h} - T_0\,. \tag{4}$$

Note that in clinical practice the inspiratory effort initiation determined when the esophageal pressure decreases by 1 $\mathrm{cmH_2O}$ [30] (and not when it starts to decrease) and is therefore shortened by 50 to 100 ms, depending on the breathing frequency. It was shown that dyspnea is reduced when the clinically measured δ_h was less than 100 ms in ventilated patients [10]: when the delay is greater than 100 ms, there is an increased patient work of breathing and a lower efficiency of ventilatory support [5]. To compensate the underestimation of δ_h in our simulations compared to clinical studies, we considered that a correct delay τ_h must be less than 200 ms.

In the present work, we considered that the inspiratory effort ends when the muscular pressure P_mus reaches 99 % of the maximum amplitude P_max: the corresponding time is designated by T_max. The triggering delay δ_l of the pressure release thus corresponds to

$$\delta_\mathrm{l} = T_\mathrm{l} - T_\mathrm{max} \tag{5}$$

where T_l is the time at which the pressure release is triggered. The delay δ_h is always positive but the delay δ_l can have a negative or a positive value, depending on whether the pressure release triggering is advanced or delayed with respect to the end of the inspiratory effort, respectively. An ideal pressure cycle would therefore mean a perfect synchronization between the beginning of the inspiratory effort and the pressure rise triggering ($\delta_\mathrm{h} < 200$ ms), and between the end of the inspiratory effort and the pressure release triggering ($|\delta_\mathrm{l}| < 300$ ms). When there is a lack of synchronization, this is, by definition, an asynchrony event. It should be clear that, sometimes, an asynchrony event can be tolerated or even wanted: for instance, in the case of patients with an acute COPD, backup cycles can be welcome. Our aim is here to assess the quality of synchronization between the breathing cycles and the pressure cycles delivered by the ventilator. We do not intend to investigate what could be the ventilator settings for an optimal assistance for a given patient. This study was conducted for helping the clinicians to know when a good "mechanical" synchronization can be obtained.

Detecting cycles and asynchrony events

Simulations were performed for each ventilator included in the protocol and data were stored for an automatic analysis using our detection algorithm working with the time series of the muscular pressure P_mus, the pressure P_v measured in the piston chamber (nearly corresponding to the pressure in the ventilatory circuit) and the mechanical lung airflow Q_p (assimilated to the patient airflow). These three time series were provided by the ASL 5000 and were filtered with a Butterworth filter acting as a low pass filter whose frequency cutoff was set at 10 Hz to reduce the measurement noise. The breathing cycles were determined by detecting time T_0 and T_max from each oscillation of the muscular pressure. During each of them, the number of times the pressure P_v becomes greater than a threshold value (equal to $\frac{P_\mathrm{h}}{2}$) allowed to determine whether this

is a non-triggered, single-triggered or double-triggered cycle (sometimes we may also observe multi-triggered cycles). All these triggerings must occur for $T_0 < T < T_{\max}$. Self-triggered (or auto-triggered) cycles were detected when the high pressure triggering occurs at time T such as $T > T_{\max}$. They were thus easily distinguished from the other types of triggered cycles. In order to detect any backup cycle (if the considered ventilator did not allow to disable this option), the duration between successive high pressure triggerings was calculated and compared to the backup frequency. Among the cycles for which the high pressure is triggered a single time during the inspiratory effort, we then computed the two delays δ_{h} and δ_{l}. When $\delta_{\mathrm{h}} \leq 200$ ms (nearly always the case) and when $|\delta_l| \leq 300$ ms, the cycle was said to be synchronous (or normal). When $\delta_{\mathrm{l}} < -300$ ms ($\delta_{\mathrm{l}} > +300$ ms), the cycle was said to be a cycle with an advanced (delayed) pressure release. The characteristics of the different types of cycles are reported in Table 3.

Once the cycles were detected and classified, various markers were computed to quantify ventilator performances. These markers are devoted to three main aspects. First, in order to characterize the high pressure triggerings, we measured the mechanical lung airflow $Q_{\mathrm{p}}(T_{\mathrm{h}})$ and the muscular pressure $P_{\mathrm{mus}}(T_{\mathrm{h}})$ at time T_{h} at which the pressure rise is triggered. We computed the triggering delay δ_{h} of the pressure rise and the lung model inspiratory work of breathing

$$W_{\mathrm{h}} = \int_{t=T_0}^{T_{\mathrm{h}}} (Q_{\mathrm{p}}(t) - Q_{\mathrm{p}}(0)) \cdot P_{\mathrm{mus}}(t)\,\mathrm{d}t \tag{6}$$

which is expressed in millijoules (mJ). Second, the pressure rise and the pressure release were evaluated as follows. We measured the actual pressure rise duration

$$\tilde{\tau}_{\mathrm{pr}} = T_{0.95P} - T_{\mathrm{h}} \tag{7}$$

between time T_{h} and time $T_{0.95P}$ at which the measured pressure P_{v} reaches 95 % of the maximum pressure of the running cycle. We computed the mean high pressure

$$\tilde{P}_{\mathrm{h}} = \frac{1}{T'_{0.95P} - T_{0.95P}} \int_{t=T_{0.95P}}^{T'_{0.95P}} P_{\mathrm{v}}(t)\,\mathrm{d}t \tag{8}$$

delivered between time $T_{0.95P}$ as previously defined and time $T'_{0.95P}$ at which the pressure returns below 95 % of the maximum pressure. This mean pressure $\tilde{P}_{\mathrm{h}}$ allowed to check whether the high pressure P_{h} set on the ventilator was actually provided. We also computed the triggering delay

$$\delta_{\mathrm{l}} = T'_{0.95P} - T_{\mathrm{ie}} \tag{9}$$

Table 3 The different types of cycles and their corresponding characteristics

Name	Symbol	N_{T}	δ_{h}	δ_{l}	
Non-triggered cycle	NT	0	—	—	
Synchronous cycle	SC	1	≤ 200 ms	$\lvert\delta_{\mathrm{l}}\rvert \leq 300$ ms	
Cycle with advanced pressure release	Tapr	1	≤ 200 ms	< -300 ms	
Cycle with delayed pressure release	Tdpr	1	≤ 200 ms	$> +300$ ms	
Self-triggered cycle	ST	1	$> \tau_{\mathrm{i}}$	—	
Backup cycle	Bck	1	—	—	$\tau_{\mathrm{tot}} = \frac{1}{f_{\mathrm{Bck}}}$
Double-triggered cycle	DT	≥ 2	—	—	

δ_{h} and δ_{l} are the delays of the high and low pressure triggerings, respectively. τ_{i} is the duration of the inspiration and τ_{tot} is the duration of the breathing cycle. N_{T} is the number of high pressure triggerings occurring during a breathing cycle. f_{Bck} is the backup frequency

of the pressure release where T_{ie} is the time at which inspiration ends and expiration starts.

Third, we computed the work $W_{0.95P}$ delivered by the ventilator during the pressure rise, that is, between time T_{h} and time $T_{0.95P}$. This marker defines the amount of ventilatory assistance provided to the lung model in response to its inspiratory effort; it characterizes the efficiency with which the high pressure level is reached. The work

$$W_{0.95P} = \int_{t=T_{\mathrm{h}}}^{T_{0.95P}} (P_{\mathrm{v}}(t) - P_{\mathrm{l}}) \cdot Q_{\mathrm{p}}(t)\, \mathrm{d}t \tag{10}$$

is expressed in Joules (J). The advantage of this work is that it characterizes the whole pressure rise and not only an arbitrary part of it. We also computed the power

$$\mathcal{P}_{0.95P} = \frac{1}{\tilde{\tau}_{\mathrm{pr}}}\, W_{0.95P} \tag{11}$$

delivered by the ventilator; it is expressed in Watt (W).

To complete these markers, we computed the minute volume

$$V_{\mathrm{m}} = V_{\max} - V_{\mathrm{R}}\,, \tag{12}$$

insufflated into the mechanical lung. Here $V_{\max}$ is the maximum volume reached during the running cycle and V_{R} is the residual volume. It allows to check whether the delivered volume per minute is greater than 8 l/min, that is, than the volume commonly required by a patient at rest.

Colored maps and synchronizability

In order to facilitate the interpretation of our measurements, we constructed maps spanned by the breathing frequency f_{b} and the mouth occlusion pressure $P_{0.1}$ by transforming the rate of detected asynchrony events (computed over 50 breathing cycles) for each pair (f_{b}, $P_{0.1}$) in a colored pixel located according to the pair ($f_{\mathrm{b}}, P_{0.1}$). The color is allocated according to the rates of the different types of asynchrony events as reported in Table 4. For instance, an indigo pixel means that more than 85 % of the cycles are synchronous, less than 10 % are cycles with advanced pressure release, less than 10 % are with delayed pressure release, less than 10 % are double-triggered and less than 10 % are non-triggered, self-triggered or backup cycles. This color thus corresponds to a very good synchronization between the breathing cycles and the ventilator pressure cycles. Contrary to this, a red pixel (compared to indigo, red is the color at the opposite end of the visible light spectrum) is associated with more than 85 % of non-triggered, self-triggered or backup cycles. We constructed our color scale (Fig. 3) assuming that cycles can be ranked according to their effect on patient's comfort as

$$\mathrm{SC} \triangleright \mathrm{Tsh} \triangleright \mathrm{DT} \triangleright \mathrm{NT}$$

where Tsh does not distinguish cycles with advanced or delayed pressure release, and NT does not distinguish non-triggered, self-triggered and backup cycles. A red pixel thus corresponds to a very poor synchronizability. Each map is made of 420 colored pixels, and provides the ability of the ventilator to synchronize its pressure cycles with the breathing cycles simulated by 420 different lung dynamics, that is, by 420 different simulated patients with a given lung mechanics.

This color scale allows to encode the gradual emergence of asynchrony events depending on the lung dynamics characterized by the pair ($f_{\mathrm{b}}, P_{0.1}$). Uniform domain corresponds

Table 4 Color legend for encoding the rates of asynchrony events computed over 50 breathing cycles for a each pair (f_b, $P_{0.1}$). Since self-triggered and backup cycles are not triggered by an inspiratory effort, there are all designated as "non-triggered" cycles

Color	SC / Tsh	Tapr	Tdpr	DT	NT
Indigo	SC $\geq$ 85 %	Tapr $<$ 10 %	Tdpr $<$ 10 %	DT $<$ 10 %	NT $<$ 10 %
Violet	Tsh $\geq$ 85 %	Tapr $<$ 85 %	Tdpr $<$ 85 %	DT $<$ 10 %	NT $<$ 10 %
Blue	Tsh $\geq$ 85 %		Tdpr $\geq$ 85 %	DT $<$ 10 %	NT $<$ 10 %
Azure	Tsh $\geq$ 85 %	Tapr $\geq$ 85 %		DT $<$ 10 %	NT $<$ 10 %
Cyan	Tsh $\geq$ 85 %			10 % $\leq$ DT $<$ 50 %	NT $<$ 10 %
Sea green	Tsh $<$ 85 %			0 % $<$ DT $<$ 50 %	NT $<$ 10 %
Green	Tsh $\leq$ 50 %			50 % $\leq$ DT $<$ 85 %	NT $<$ 10 %
Lime	Tsh > NT			DT $<$ 50 %	10 % $\leq$ NT $<$ 85 %
Yellow				DT $\geq$ 85 %	
Orange	Tsh $\leq$ NT		or	50 % $\leq$ DT $<$ 85 %	10 % $\leq$ NT $<$ 85 %
Red					NT $\geq$ 85 %

SC = synchronous cycle, Tapr = cycle with an advanced pressure release, Tdpr = cycle with a delayed pressure release, Tsh = Tdpr or Tapr, DT = double-triggered cycles, NT = non-triggered cycle or self-triggered cycle or backup cycle
Each color is allocated according to various thresholds on the rates of asynchrony events as reported in the table

to a stable behavior of the ventilator with given rates of asynchrony events. When various colors (not close each other in the spectrum) co-exist in a neighborhood (more or less like in a patchwork), this means that there is an instability in the interactions between the lung model and the ventilator, that is, one may expect that in such a situation with a real patient, the type of cycles could significantly change in a short duration (a real patient always breathes with a cyclic dispersion in the breathing frequency and in the occlusion pressure). When the color changes in a smooth way (according to the color spectrum), this means that the domain for which the ventilator works well is rather well defined: it is thus possible to state without any ambiguity for which (sub-) cohort of simulated patients, the ventilator can be recommended.

To quantify the global ventilator synchronizability over a map, that is, for a cohort of simulated patients with a given lung mechanics (obstructive, restrictive or normal) and for a given set of values for ventilator parameters, we computed a synchronizability $\varepsilon_{\tilde{f}_b,\tilde{P}_{0.1}}$ (where $\tilde{f}_b$ and $\tilde{P}_{0.1}$ are the discrete values retained for varying the breathing frequency and the occlusion pressure, respectively) which takes into account the number of each type of cycles as

$$\varepsilon_{\tilde{f}_b,\tilde{P}_{0.1}} = 1 - \frac{1}{N_c}\sum_{n=1}^{N_c} e_n \tag{13}$$

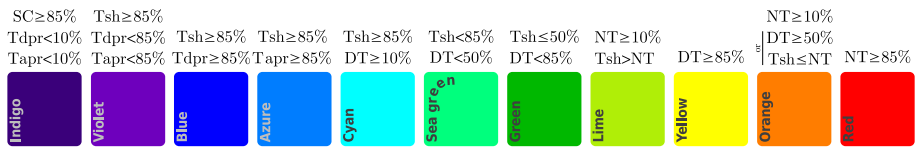

Fig. 3 Color scale. This color scale is used to encode the rates of asynchrony events counted for each pair (f_b, $P_{0.1}$). Indigo (*left end of the spectrum*) represents an excellent synchronizability which is gradually deteriorated as the color changes toward the red (*right end of the spectrum*) corresponding to a very poor synchronizability

where N_c is the number of breathing cycles simulated ($N_c = 50$ in our case) and

$$e_n = \begin{cases} 0 & \text{if the } n\text{th cycle is SC} \\ \frac{1}{4} & \text{if the } n\text{th cycle is Tapr or Tdpr} \\ \frac{1}{2} & \text{if the } n\text{th cycle is DT} \\ 1 & \text{if the } n\text{th cycle is NT.} \end{cases}$$

Synchronizability $\varepsilon_{\tilde{f}_b, \tilde{P}_{0.1}}$ is thus equal to 1 when the ventilator pressure cycles are well synchronized with the breathing cycles (100 % of synchronous cycles). This synchronizability is decreased as the number of asynchrony events increases. A mean synchronizability is then computed for each map according to

$$\varepsilon = \frac{1}{N_{\tilde{f}_b} \times N_{\tilde{P}_{0.1}}} \sum_{i=1}^{N_{\tilde{f}_b}} \sum_{j=1}^{N_{\tilde{P}_{0.1}}} \varepsilon_{ij}\,, \tag{14}$$

where (i, j) represent the pair of discrete values of $(f_b, P_{0.1})$ characterizing the lung dynamics; $N_{\tilde{f}_b}$ and $N_{\tilde{P}_{0.1}}$ are the numbers of values retained for the breathing frequency f_b and the occlusion pressure $P_{0.1}$ for constructing the colored map, respectively. In our case, $N_{\tilde{f}_b} = 21$ and $N_{\tilde{P}_{0.1}} = 20$, inducing $21 \times 20 = 420$ pixels in each map.

A synchronizability ε close to 1 (100 %) corresponds to an excellent synchronization of the ventilator pressure cycles with the breathing cycles provided by the mechanical lung; when ε is about 0, this means that there are many asynchrony events.

Comparative results

Our results were averaged over the five parameter settings tested for each ventilator (the maximum high pressure triggering sensitivity versus the minimum, median and maximum pressure rise duration, and the minimum pressure rise duration versus the minimum and median high pressure triggering sensitivity). To compare ventilators performances which depend on the lung model to which they are connected, we performed a normality test (Shapiro-Wilk) to check whether the markers were normally distributed, with a statistical significance set at $p < 0.05$. If the test was negative, a Wilcoxon rank-sum test was performed to determine if one distribution was stochastically greater than the other. If the test was positive, a Student t-test (if the variances between the two distributions were equal) or a Welch t-test (if the variances were different) was performed to determine whether the two sets of data were significantly different from each other. In order to assess the disparities in terms of synchronizability and performances between the different ventilators, we performed a Kruskal-Wallis rank-sum test, which is the non-parametric equivalent of the ANOVA test, to test whether samples originate from the same distribution.

Results

This procedure was applied to eight recent domiciliary ventilators: the BiPAP A40 (Philips Respironics), Elisée 150 (ResMed), Monnal T50 (Air Liquide Medical Systems), S9 VPAP ST (ResMed), SomnoVENT autoST (Weinmann), Stellar 100 (ResMed), Trilogy 100 (Philips Respironics), Vivo 50 (Breas), and an older one, the Smartair ST (Covidien).

Selected values of the settings for these ventilators are reported in Table 2. All the ventilators were tested in a barometric regulation (the pressure is controlled), even when other regulations are available.

Synchronizability ε

The ability of a ventilator to synchronize the pressure cycles they deliver with the simulated breathing cycles depends on the lung model used: the mean synchronizability was significantly ($p < 0.05$, Wilcoxon rank-sum test) smaller with the restrictive model ($\overline{\varepsilon} = 56.6 \pm 26.5$ %) than with the obstructive model ($\overline{\varepsilon} = 68.6 \pm 24.7$ %).

As shown in Fig. 4, performances are different from a ventilator to another, as confirmed by the Kruskal-Wallis rank-sum test ($p < 0.01$ for both restrictive and obstructive lung models) which indicates that the synchronizabilities computed for the nine ventilators do not belong to a unique distribution. With the restrictive model, the Vivo 50 and SomnoVENT autoST have a maximum synchronizability greater than 90 %, that is, close to an optimal synchronization with the pulmonary model. Contrary to this, the S9 VPAP ST and Stellar 100 have minimum synchronizability equal to 0 % with the largest high pressure triggering sensitivity and the smallest pressure rise duration. With the obstructive model, the BiPAP A40, Elisée 150 and Trilogy 100 have the best performances and present a maximum synchronizability greater than 90 %. The Monnal T50 and Smartair ST present a very poor synchronizability for low sensitivities of the pressure rise triggering when connected to this lung mechanics.

Asynchrony events

With the restrictive model, self-triggered cycles are the asynchrony events which mostly reduce the synchronizability. These cycles were encountered with more than 50 % of the ventilators tested, mainly for the large sensitivities of the high pressure triggering. This is observed with the Monnal T50, S9 VPAP ST, Stellar 100, BiPAP A40, Trilogy 100 and SomnoVENT autoST (Fig. 5). Double-triggered cycles may also happen and reduce the synchronizability; they were observed with the S9 VPAP ST, Stellar 100 and for a few ventilatory dynamics in the case of the Vivo 50. These two asynchrony events were due to a large pressure rise triggering sensitivity; consequently, there are more pressure cycles delivered than required by the simulated breathing cycles.

With the obstructive model, the time constant (equal to RC) of the lung model is large and induces slow variations in the airflow Q_{p}. Detecting the inspiratory effort may therefore be difficult as evidenced by the numerous non-triggered cycles we detected, especially with the Monnal T50, Smartair ST and to a lesser extent, with the Vivo 50. Most of the time, small sensitivities of the high pressure triggering lead to ineffective inspiratory efforts from the lung model.

Triggering performances

Mean delays $\overline{\delta}_{\mathrm{h}}$ (Fig. 6) were significantly ($p < 0.01$, Welch t-test) shorter with the restrictive model ($\overline{\delta}_{\mathrm{h}} = 131 \pm 27$ ms) than with the obstructive model ($\overline{\delta}_{\mathrm{h}} = 187 \pm 41$ ms). The Vivo 50 and Trilogy 100 had the shortest triggering delays of the pressure rise

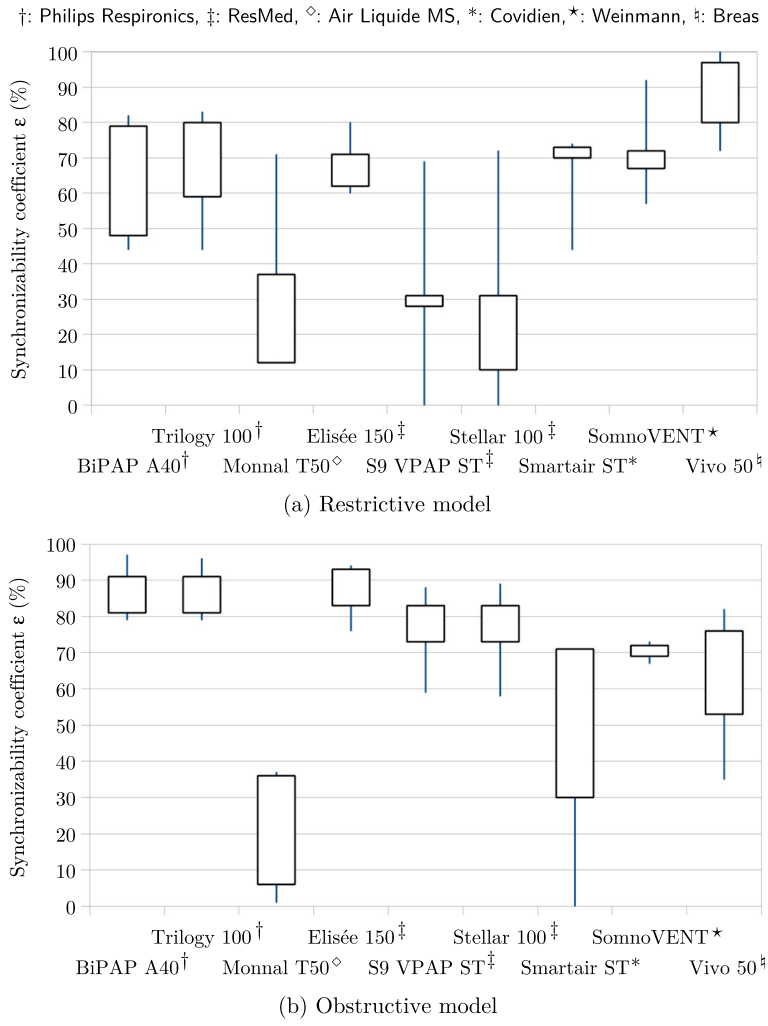

Fig. 4 Box plot representation of the synchronizabilities. Synchronizabilities computed for the ventilators connected to the restrictive (**a**) and obstructive **b** models for all different settings. Bottom and top of the box are the first and third quartiles, whereas ends of the whiskers are the minimum and maximum values

($\leq$ 100 ms) with the restrictive model, whereas the Smartair ST presented the longest delay ($>$ 170 ms). The Monnal T50 and SomnoVENT autoST had good triggering performances with the obstructive model since the delays $\overline{\delta}_{\mathrm{h}}$ were less than 140 ms with these two devices. The BiPAP A40, S9 VPAP ST, Stellar 100, Trilogy 100 and Vivo 50 presented the largest triggering delays ($\delta_{\mathrm{h}} > 200$ ms).

Triggering delays of the pressure rise measured with the restrictive lung mechanics are significantly ($p = 0.015$, Student t-test) different from those measured with the obstructive model (Fig. 7).

In other words, when a device has small (large) delays with the restrictive model, it has large (small) delays with the obstructive model. This indicates that when the triggering strategy developed by a manufacturer for a ventilator is efficient for one lung mechanics, it might not perform as well for the second one. Some ventilators may therefore be more dedicated to a type of pulmonary disease than others.

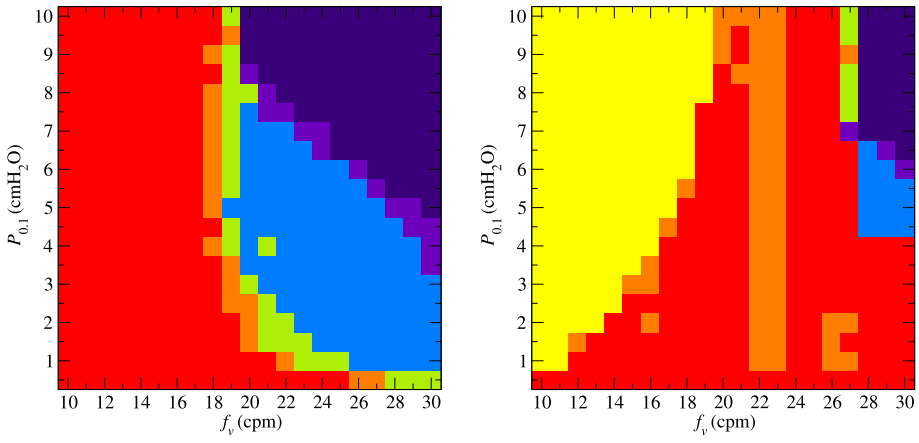

Fig. 5 Colored maps showing the incidence of two asynchrony events. Incidence of self-triggered cycles (*lime, orange, red pixels*) and double-triggered cycles (*yellow pixels*) for two ventilators connected to the restrictive lung model

The mechanical lung work of breathing W_h to trigger the pressure rise was significantly ($p < 0.05$, Welch t-test) greater, in absolute value, for the obstructive model ($\overline{W}_h = -2.26 \pm 1.66$ mJ) than for the restrictive model ($\overline{W}_h = -0.72 \pm 0.62$ mJ). It reveals that the longer delay required to detect the simulated inspiratory efforts for triggering the pressure rise with the obstructive model may induce an increase of the work of breathing and, consequently, a less effective unloading of the respiratory muscles.

The airflow Q_p and the pressure P_{mus} at the time T_h the pressure rise is triggered were computed. Nevertheless, no statistical test was possible due to some configurations for which asynchrony events were too frequent and led to a synchronizability close to 0. The measured airflows were consistent with the announced values for the BiPAP A40 and Trilogy 100 whose triggering sensitivities are provided in l/min. No direct correspondence

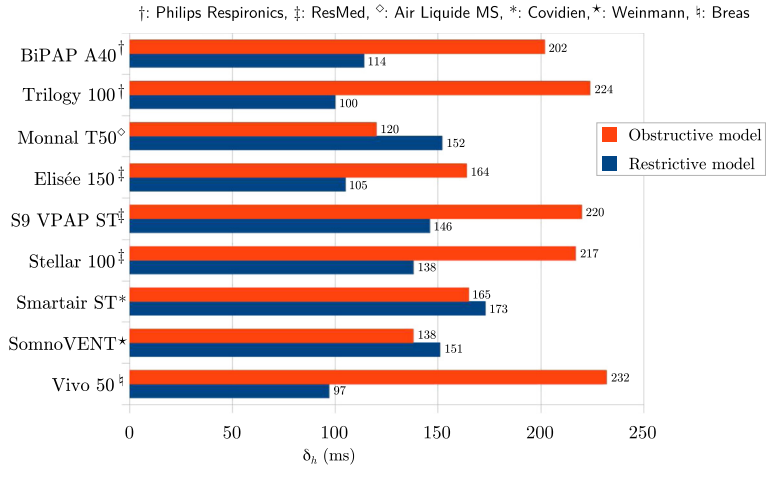

Fig. 6 High pressure triggering delays $\overline{\delta}_h$. Mean delays δ_h for the nine ventilators (for their respective maximum high pressure triggering sensitivity) connected to the restrictive and obstructive models

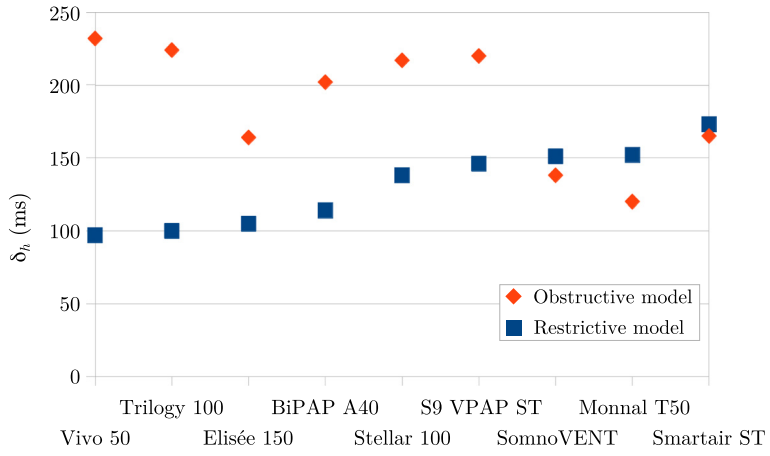

Fig. 7 Mean triggering delays $\overline{\delta}_h$ ranked in ascending order. High pressure triggering delays measured with a restrictive lung mechanics (*blue*) ranked in ascending order and correspondence with an obstructive mechanics (*red*)

was found for the other ventilators and such assessment was impossible to perform when the triggering sensitivities were given without any unit or qualitatively as in the S9 VPAP ST or the Stellar 100. This is the main reason for which it is rather difficult to compare the performances of the different ventilators. In order to distinguish different strategies for triggering the pressure rise, we plotted the mechanical lung airflow and the muscular pressure at the time the pressure rise is triggered (versus an index designating each pair $(f_b, P_{0.1})$ by an integer between 1 and 420) (Fig. 8). These curves provide patterns which allow us to classify the ventilators in three groups, suggesting similar response from the ventilators for a given group in the cohort of simulated patients. These different patterns explain why it is difficult to reliably compare triggering performances in different ventilators.

With the restrictive model, the minimum airflow required to trigger the pressure rise with the lowest sensitivity is large for the Monnal T50 ($Q_p \geq 47.8$ l/min, corresponding to $P_{mus} \leq -8.5$ cmH$_2$O) and Smartair ST ($Q_p \geq 46.2$ l/min, $P_{mus} \leq -8.2$ cmH$_2$O). It explains the numerous non-triggered cycles observed when these ventilators are connected to the restrictive model. To a lesser extent, the required airflow was quite large with the Vivo 50 ($Q_p \geq 18.3$ l/min, $P_{mus} \leq -3.9$ cmH$_2$O) for the minimal triggering sensitivity of the pressure rise.

With the obstructive model, the non-triggered cycles with the Monnal T50 and Smartair ST were so frequent that it was not possible to correctly compute the mechanical lung airflow Q_p or the muscular pressure P_{mus} when the pressure rise is triggered. In fact, these minimum triggering sensitivities for the pressure rise which are available on these two devices seem to be not clinically pertinent. The required airflow was quite large with the Vivo 50 ($Q_p \geq 20.8$ l/min, $P_{mus} \leq -13.3$ cmH$_2$O) connected to the obstructive lung model.

Pressure rise and return pressure release

For the restrictive model, the effective pressure rise duration $\tilde{\tau}_{pr}$ depends on the ventilator and, for a given device, depends on the lung model (Fig. 9). For the restrictive mechanics,

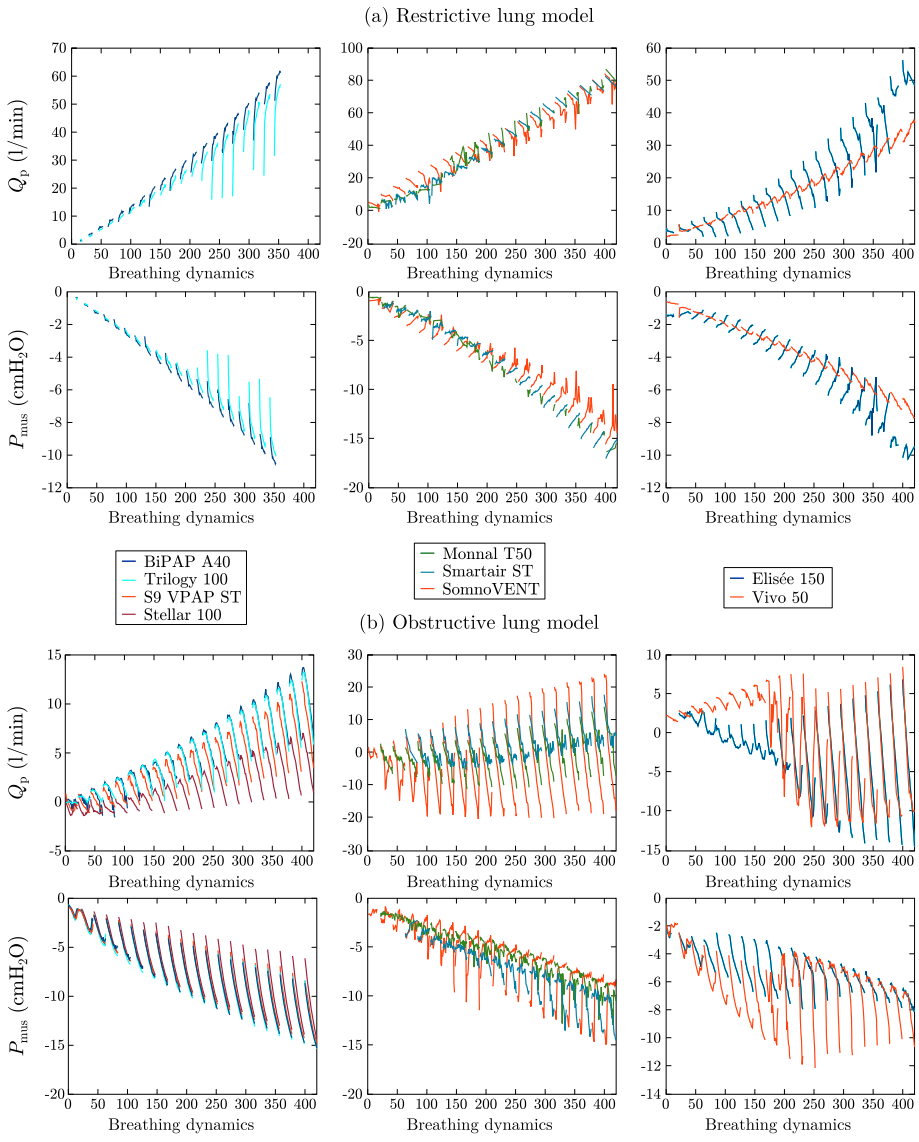

Fig. 8 Mechanical lung airflow and muscular pressure at high pressure triggering. Mechanical lung airflow Q_p and muscular pressure P_{mus} measured at time T_h at which the pressure rise is triggered, for every breathing dynamics tested. Each segment represents the values measured for one given $P_{0.1}$ (*increasing from the left to the right*) and all breathing frequencies. All ventilators were set to the maximum pressure rise triggering sensitivity

the mean pressure rise duration was between 326 ± 99 ms and 598 ± 184 ms, corresponding to a mean range of 272 ms. Three ventilators presented a range less than 100 ms, that is, reduced possibilities to adapt the pressure rise to the lung dynamics: the Monnal T50 ($404 < \tilde{\tau}_{pr} < 420$ ms), Smartair ST ($426 < \tilde{\tau}_{pr} < 507$ ms) and SomnoVENT autoST ($486 < \tilde{\tau}_{pr} < 507$ ms). The S9 VPAP ST and Stellar 100 had the widest range of pressure rise durations ($222 < \tilde{\tau}_{pr} < 931$ ms and $213 < \tilde{\tau}_{pr} < 860$ ms, respectively) and a linear scale expressed in seconds which corresponds to the measured values, being therefore easy to use.

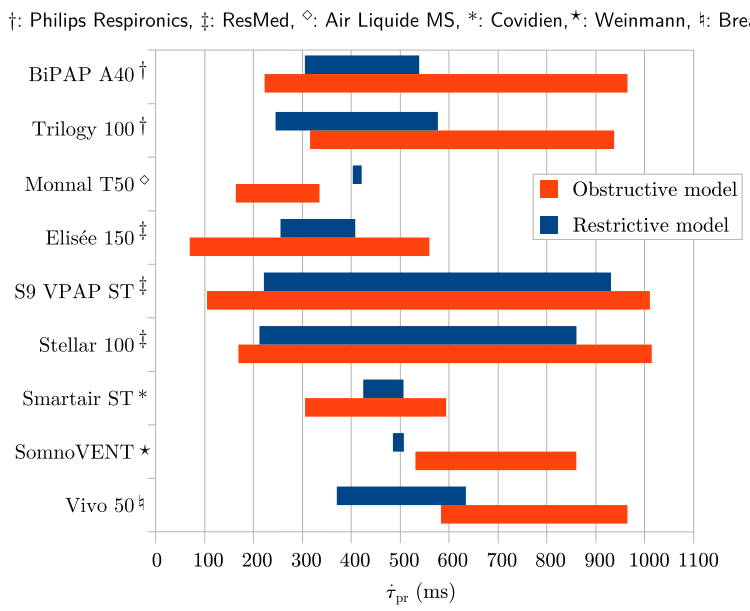

Fig. 9 Mean pressure rise duration $\tilde{\tau}_{pr}$. Range of the pressure rise duration $\tilde{\tau}_{pr}$ measured for the nine ventilators connected to the restrictive (*blue*) and obstructive (*red*) lung models when the corresponding parameter is set to its smallest and largest values

For the obstructive model, the mean pressure rise duration $\tilde{\tau}_{pr}$ was between 274 ± 181 ms and 805 ± 247 ms, that is, a mean range of 531 ms which is greater than the one measured with the restrictive model. Measured ranges are small with the Monnal T50, Smartair ST, SomnoVENT autoST and Vivo 50 (less than 400 ms), and wide with the S9 VPAP ST ($105 < \tilde{\tau}_{pr} < 1012$ ms) and Stellar 100 ($169 < \tilde{\tau}_{pr} < 1016$ ms), as well as with the BiPAP A40 ($223 < \tilde{\tau}_{pr} < 966$ ms). The S9 VPAP ST and Stellar 100 (both from ResMed) are the only two ventilators for which the measured pressure rise durations are identical with the restrictive and obstructive lung models, which roughly correspond to the announced settings (given in ms).

The triggering delay δ_l of the pressure release is most often negative with the restrictive model ($\overline{\delta_l} = -171$ ms for the nine ventilators and the five parameter settings). It is positive with the obstructive model ($\overline{\delta_l} = +233$ ms), as reported in [33]. The synchronization with the end of the inspiratory effort mostly depends on the pressure rise duration and on the ventilator ability to estimate the airflow actually delivered to the patient. Pressure release triggerings were particularly advanced ($\overline{\delta_l} = -480$ ms) with the Elisée 150 connected to the restrictive model, meaning that cycles with advanced pressure release frequently occurred, even with the longest pressure rise duration (Fig. 10a). Contrary to this, delays $\overline{\delta_l}$ were large with the SomnoVENT autoST connected to the obstructive model ($\overline{\delta_l} = 646$ ms), leading to numerous cycles with delayed pressure release, even with the shortest pressure rise duration (Fig. 10b).

The mean pressure rise duration leading to the smallest triggering delay ($\overline{\delta_l} = -42 \approx 0$ ms) of the pressure release, and thus corresponding to an optimal synchronization with the end of the inspiratory effort, was equal to 511 ms for the restrictive model, and equal to 297 ms ($\overline{\delta_l} = +182 < +300$ ms) for the obstructive model. These measured pressure

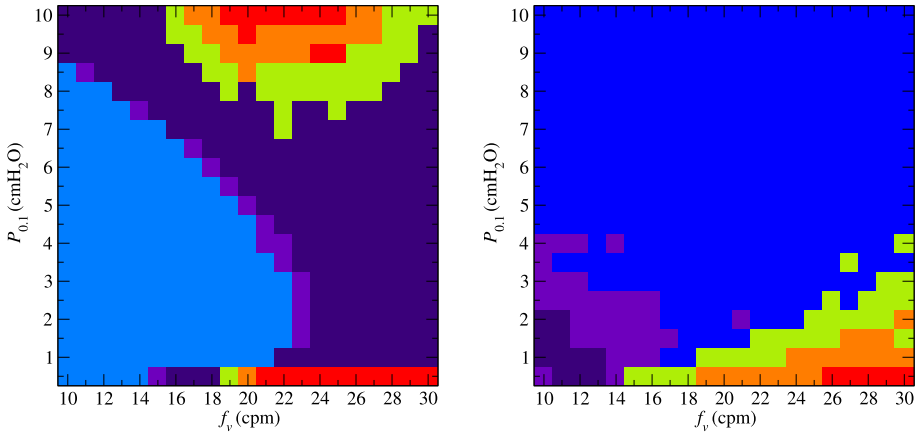

Fig. 10 Colored maps with pressure release asynchrony events. Two maps showing the incidence of cycles with advanced pressure release (*azure domain in the bottom left part*) with the Elisée 150 connected to the restrictive mechanics (**a**) and of delayed pressure release (*blue domain in the top part*) with the SomnoVENT autoST connected to an obstructive mechanics (**b**)

rise durations were significantly different ($p < 0.01$, Welch t-test) between the two lung mechanics.

When connected to the obstructive model, the mean high pressure actually delivered to the mechanical lung was close to the preset value for all the ventilators. With the restrictive model, the measured high pressure $\tilde{P}_h$ may strongly depend on the selected pressure rise duration τ_{pr}, as exemplified with the A40 and Trilogy 100: for these two ventilators with the most sensitive high pressure triggering and the longest pressure rise duration, the measured pressure $\tilde{P}_h$ are 14.8 cmH_2O and 15.7 cmH_2O, respectively. This represents, compared to the preset value $P_h = 20$ cmH_2O, a lack of 5.2 and 4.3 cmH_2O, respectively. This likely means that what is selected on these two devices (from the same manufacturer) is in fact the derivative of the pressure, $\frac{dP_h}{dt}$ (a slope as suggested by the translation in the French version, "pente"): when it is too small, the pressure release occurs before the preset value P_h is reached. This is therefore a good example of the ambiguity which can occur with the heterogeneity in the variable settings and strategies. In principle, the physician would expect that the preset high pressure is reached before the pressure release is triggered, a feature which is rather difficult to check prior to any monitoring since neither the duration of the high pressure phase τ_h nor the pressure rise duration τ_{pr} (in ms) are known. The A40 has a measured pressure rise duration which varies between 306 and 538 ms when connected to the restrictive model and, between 233 and 966 ms when connected with the obstructive model (rather similar values were measured with the Trilogy 100). The booklet corresponding to these two ventilators announced a pressure rise duration between 100 and 600 ms. In fact, in spite of its English name "rise time", used in these two ventilators, we cannot be ensured that this parameter is actually a duration since the manufacturer translated it by "pente" (slope) in French, thus justifying why the pressure rise durations were measured within a so wide range, contrary to what was observed

with the S9 VPAP ST and the Stellar 100. Further measurements should be performed to determine what is exactly set with this parameter.

Contrary to what was observed when connected to the obstructive model, the mean pressure delivered was greater than the preset value with the Elisée 150, Smartair ST and SomnoVENT autoST (for all parameter settings): we thus measured $\overline{\tilde{P}}_h = 22.7$ cmH$_2$O, $\overline{\tilde{P}}_h = 23.0$ cmH$_2$O and $\overline{\tilde{P}}_h = 24.1$ cmH$_2$O, respectively.

Ventilators pressurization performances

The mean power $\overline{\mathcal{P}}_{0.95P}$ delivered by the ventilators was significantly ($p < 0.01$, Wilcoxon rank-sum test) greater with the restrictive lung mechanics ($\overline{\mathcal{P}}_{0.95P} = 1.09 \pm 0.24$ W) than with the obstructive lung mechanics ($\overline{\mathcal{P}}_{0.95P} = 0.50 \pm 0.12$ W). This is in agreement with the fact that more work is required to inflate the lungs when compliance is reduced. This power is strongly correlated to the delivered pressure $\tilde{P}_\mathrm{h}$. In order to evidence such a relationship, we compared the difference in the mean pressure $\Delta\overline{P}_\mathrm{h}$ delivered by the ventilators connected to the restrictive lung models when the pressure duration is equal to its shortest and longest values (Fig. 11) to the mean relative power $\Delta\overline{\mathcal{P}}_\mathrm{h}$ in the same conditions. These two quantities are strongly correlated ($\rho = 0.87$, $p < 0.01$, Pearson's product-moment correlation). Due to a very limited range for varying the pressure rise duration (as observed in the Monnal T50 and the SomnoVENT autoST), some ventilators do not offer a wide range of possibilities in the support delivered to the lung model when this parameter is varied.

Minute volume V_m

The mean minute volume insufflated to the lung model was significantly ($p < 0.01$, Welch t-test) greater when the ventilators were connected to the restrictive lung model ($V_\mathrm{m} = 12.5$ l/min) than when they were connected to the obstructive one ($V_\mathrm{m} = 10.9$ l/min). No significant difference was observed among the mean minute volume delivered by the different ventilators.

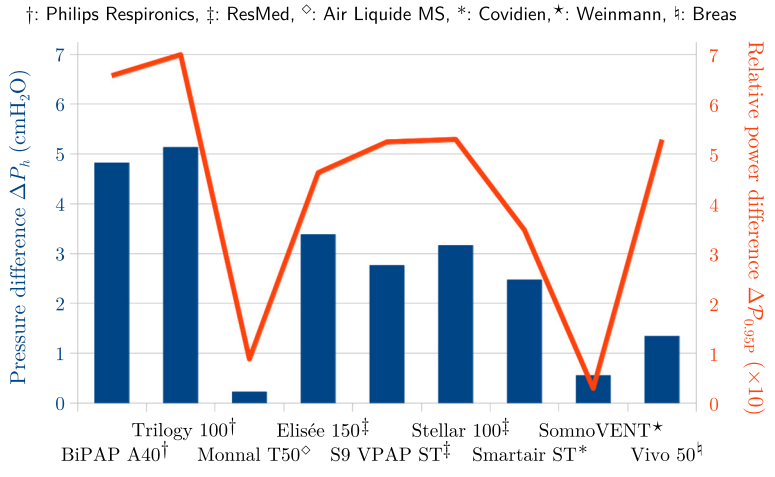

Fig. 11 Link between high pressure and power delivered. Differences (in absolute value) in the pressure delivered by the ventilators connected to the restrictive model when the pressure rise duration is the shortest and the longest (*blue bars*). Differences in the power delivered in the same conditions (*red line*) are also drawn

Discussion

The main limitation of the present study is that ventilators were tested with a mechanical lung which does not fully behave like the human respiratory system. In particular, the pressure support delivered by the ventilator has no feedback on the lung dynamics. However, patient's inspiratory efforts were modeled in a realistic way and should therefore be considered as actually representative of the physiological breathing dynamics. Moreover, the ASL 5000 is a mechanical lung which was already used by other investigators for ventilator benchmarking [15–19]. Another limitation is that our ventilatory circuit was built with a constant and calibrated leak whereas noninvasive ventilation is often associated with non-intentional leaks around the mask that may vary in time. Another series of tests will be therefore performed (and discussed elsewhere) with a device allowing non-intentional and variable leaks during pressure support, in order to better reflect ventilator behaviour in more realistic conditions. This is particularly important because the ventilator software have very different performances in accounting for a non-intentional leak and they may induce additional asynchrony events in doing that. A last limitation is due to the disparities inherent to the different strategies developed by the manufacturers to drive their ventilators: this makes some comparisons difficult to establish as previously explained. In this study, we defined a parametric procedure allowing to test the ventilators connected to a large cohort of simulated patients (and not a single one) and therefore providing reliable evaluations of the markers we introduced. It should be clear that our aim is not to provide the best parameter settings for a given patient but rather to assess how easy it is to obtain a good synchronization between the breathing cycles and the pressure cycles delivered by the ventilator. Indeed, a large "indigo" domain means that a patient with a similar lung mechanics but whose lung dynamics (characterized by the ventilatory frequency and the occlusion pressure) slightly changes will remain well synchronized with the pressure cycles delivered by the ventilator.

This bench model study highlighted the disparities existing in the abilities of nine domiciliary ventilators to synchronize with various simulated patients. Our results suggest that some ventilators are better designed to answer the demand of certain lung mechanics than others. For instance, the Vivo 50 and SomnoVENT autoST have excellent results when connected to the restrictive model and the BiPAP A40, Elisée 150 and Trilogy 100 when connected to the obstructive model (Fig. 12). These departures in the observed performances — at least partly — explain why clinicians may encounter some difficulties to adequately set a given ventilator for patients with a type of pulmonary disorders and not for patients with another type of pathology. The asynchrony events encountered during the simulations were rather characteristic of a given lung mechanics, due to the breathing dynamics which strongly differs between restrictive and obstructive conditions. With a restrictive model, fast variations in the patient airflow (related to the short time constant of his respiratory system) can lead to self-triggered cycles when the triggering sensitivity of the pressure rise is too large. A particular attention should be therefore paid to set a suitable triggering sensitivity of the pressure rise to avoid these asynchrony events. Contrary to this, the slow variations in the patient airflow with obstructive conditions may result in non-triggered cycles. Large sensitivities of the pressure rise triggering should therefore be preferred. Nevertheless, in the latter case, the disparities existing between the ventilators can make such an adjustment difficult to obtain since the triggering strategies, as well as the units (when they are provided), differ from a device to another one. Even for

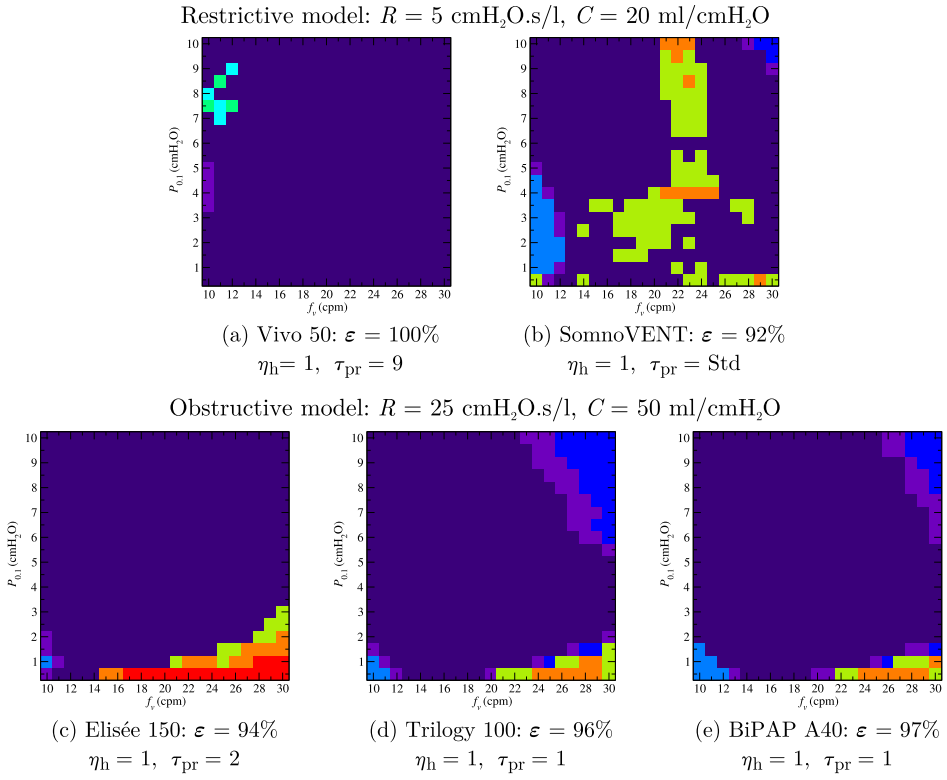

Fig. 12 Colored maps with excellent synchronizabilities. Examples of maps computed for ventilators presenting an excellent synchronizability with the restrictive (**a** and **b**) and with the obstructive model (**c**, **d** and **e**)

the pressure rise triggering sensitivities, expressed in l/min, the correspondence with the actual patient airflow is not direct and can lead to misunderstandings (for instance, the airflow measured (28.0 l/min) at time T_h when the pressure rise is triggered is significantly larger than the preset airflow ($\eta_h = 5$ l/min) in the Monnal T50 connected to a restrictive lung mechanics. The synchronizability maps computed for the maximum, median and minimum pressure rise triggering sensitivities are therefore particularly relevant since they allow to compare objectively the triggering performances of the ventilators. When the mouth occlusion pressure $P_{0.1}$ and the breathing frequency f_b of a patient with restrictive or obstructive disorders are known, it should be possible to check whether a ventilator can synchronize correctly its pressure cycle with the breathing cycles of the lung model for such a pair $(f_b, P_{0.1})$.

By measuring the triggering delay of the pressure rise, we highlighted the important inter-ventilator variability for detecting the inspiratory efforts: the BiPAP 40, Elisée 150, Trilogy 100 and Vivo 50 are efficient with the restrictive lung mechanics whereas the Monnal T50 and SomnoVENT autoST presented good performances with the obstructive lung mechanics. Most likely, different triggering strategies can explain such disparities, some ventilators (as, for instance, the Vivo 50, Trilogy 100, Stellar 100, Elisée 150 and BIPAP 140) being excellent with the restrictive lung mechanics but significantly worse with an obstructive mechanics. Some others are good with both types of lung mechanics (the Monnal T50, SommnoVENT autoST and Smartair ST) (Fig. 9). Some triggering strategies are therefore quite specific to a type of pulmonary disease.

From the measures performed on pressure rise duration, it was shown that long pressure rise durations led to more synchronous cycles with a restrictive lung mechanics whereas short durations better suit the obstructive lung mechanics. Such a feature could explain why some ventilators do not synchronize properly; indeed, a too tight range for the pressure rise durations (as observed in the Monnal T50 and the SomnoVENT autoST with the restrictive mechanics) does not allow to have the value required for the considered lung mechanics. Consequently, comparing the minimum, median and maximum pressure rise durations for each ventilator allows to quickly assess the effect of this setting on the synchronization between the breathing cycles and the ventilator pressure cycles.

We showed that all ventilators actually deliver the preset pressure value when connected to the obstructive mechanics. Contrary to this, when connected to the restrictive mechanics, the pressure actually delivered is significantly less than the preset value (BiPAP A40, Trilogy 100). Nevertheless, no major effect was observed in the delivered minute volume V_{m}.

Our choices for the pressure release triggering sensitivity η_{l} according to the lung mechanics (around 25 % for the restrictive model and around 75 % for the obstructive one) could have been optimized by increasing it for the restrictive lung mechanics and by decreasing it with the obstructive mechanics since we observed cycles with advanced pressure release in the former case and cycles with delayed pressure release in the latter case. A further study could be performed in varying this parameter in order to rigorously investigate its influence on patient-ventilator synchronization.

We provided all parameters required to reproduce the tests we performed in this study. We introduced a terminology to distinguish the patient (or mechanical lung) breathing cycles from the ventilator pressure cycles, a key point to clearly describe all the observed events. The present procedure was developed to compare different ventilators in pressure support mode. Most of this procedure can be straightforwardly extended to other ventilation modes or types of ventilators. This parametric procedure can be also used to investigate the evolution of the performances provided by various version of a given device (improved from a mechanical and/or an algorithmic point of view). As an example, we compared the synchronizability ε computed for the Vivo 40 (Breas) and two different software versions dedicated to the Vivo 50: initially poor ($\varepsilon = 10$ %, see Fig. 13a), the synchronizability progressively increases ($\varepsilon = 84$ %, Fig. 13c) mainly, in this case, because the

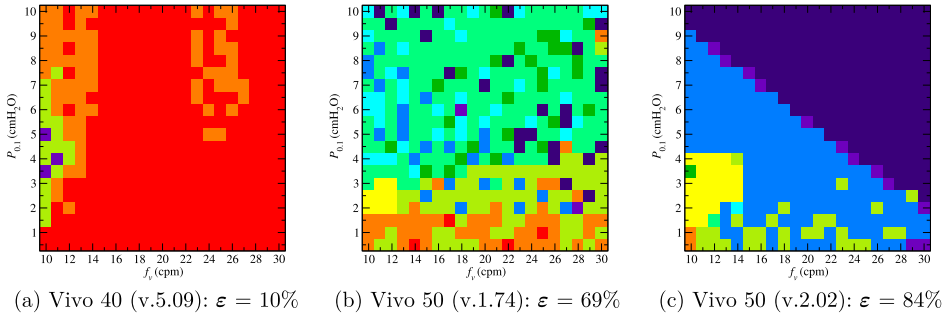

(a) Vivo 40 (v.5.09): $\varepsilon = 10\%$ (b) Vivo 50 (v.1.74): $\varepsilon = 69\%$ (c) Vivo 50 (v.2.02): $\varepsilon = 84\%$

Fig. 13 Evolution of the synchronizability. Synchronizability computed for some of the devices produced by Breas, that is, the Vivo 40 and the Vivo 50 with two different versions of its software. The three devices were connected to the restrictive model with $\eta_{\mathrm{h}} = 1$ and $\tau_{\mathrm{pr}} = 1$. Self-triggered cycles (*lime, orange, red pixels*) were gradually replaced by synchronous cycles (*indigo pixels*) or cycles with advanced pressure release (*azure pixels*)

rate of self-triggered cycles decreases, these cycles being replaced by synchronous cycles, once an intermediate unstable device was produced (Fig. 13b). Indeed, heterogeneous synchronizability map as the one observed with the Vivo 50 equipped with the software, version 1.74 (Fig. 13b) is the signature of a control loop which can be easily in conflict with itself.

Conclusion

This work was first devoted to develop a new parametric procedure for testing performances of devices used in mechanical ventilation. The main improvement is that the ventilators were tested for a large cohort of 420 simulated lung dynamics. This allows to take into account the inter-patient variability and, consequently, to provide a rather reliable evaluation of the ventilators performances. By performances, we mainly focused our attention on the ability presented by the ventilators to synchronize their pressure cycles with the breathing cycles simulated by the mechanical lung. The synchronizability we computed thus assesses the ability of the ventilator to correctly answer the inspiratory demand in synchronizing the phase during which the high pressure is delivered with the inspiration (here simulated with a mechanical lung). The clinician who has to treat a patient whose lung mechanics and dynamics can change in time is helped by our results in the sense that he may check whether his patient is in the middle of an indigo domain rather than in a red domain. Thus a slow and/or limited change in his patient physiological or pathological state would not affect too much the synchronization between the patient breathing cycles and the pressure cycles delivered by the ventilator.

In order to adjust the parameter settings depending on the lung mechanics, it is widely accepted that the sensitivity for the pressure release must be around 25 % for a restrictive lung mechanics and around 75 % for an obstructive one. We used these "common" parameter values in our study. According to our results, the most critical parameter is the high pressure triggering sensitivity η_{h}. Indeed, for seven of the nine ventilators tested, the best synchronizabilities were obtained by choosing for obstructive lung mechanics more sensitive triggers for the pressure rise than for restrictive mechanics. Contrary to this, the most sensitive trigger must be used with the Elisée 150 and the Vivo 50. The pressure rise duration τ_{pr} is influent for these two devices as well as for the Monnal T50. For the

Table 5 Values of the two parameters (high pressure triggering sensitivity η_h and pressure rise duration τ_{pr}) maximizing the synchronizability ε according to the pulmonary model considered. These values were obtained from the tests performed under the protocol we defined and do not imply that a better combination of settings can not be found. The pressure release triggering sensitivity η_{l} is also reported

	Restrictive model				Obstructive model			
	η_{h}	τ_{pr}	η_{l}	ε	η_{h}	τ_{pr}	η_{l}	ε
BiPAP A40	5 l/min	1	25 %	82 %	1 l/min	1	75 %	97 %
Elisée 150	1	4	25 %	80 %	1	2	75 %	94 %
Monnal T50	5 l/min	1	25 %	71 %	0.5 l/min	4	75 %	37 %
S9 VPAP ST	Very low	Min	Very low	69 %	Very high	Min	Very high	88 %
Smartair ST	3	1	–75 %	74 %	1	1	–25 %	71 %
SOMNOvent	1	Std	—	92 %	–1	Std	—	73 %
Stellar 100	Very low	MIN	Very low	72 %	Very high	MIN	Very high	89 %
Trilogy 100	5 l/min	1	25 %	83 %	1 l/min	1	75 %	96 %
Vivo 50	1	9	7	100 %	1	1	3	82 %

two formers, most likely this parameter balances the lack of effect induced by changing the triggering sensitivity. In the latter (the Monnal T50), the logic is inverted compared to other ventilators: a larger τ_{pr} is obtained with a smaller parameter value, most likely because it quantifies the slope of the pressure rise, and not its duration. When a clinician has a restrictive patient to treat, a Vivo 50 or a SOMNOvent autoST should be very easy to synchronize. When an obstructive patient is considered, a Respironics or an Elisée 150 could allow an easy synchronization. When a rather small synchronizability is obtained, this means that the number of parameter values for which a good synchronization is observed is smaller and, consequently, more difficult to find. The parameter values maximizing the synchronisability ε according to the pulmonary mechanics for each tested ventilator are reported in Table 5. Consequently, it can not be said that a given ventilator is better than another one without specifying the lung mechanics and dynamics: the ventilator must therefore be carefully chosen for each patient. It is hoped that the synchronizability maps provided by such a study could be useful for guiding the clinician in his choice.

Competing interests
The authors declare that they have no competing interests.

Authors' contributions
EF and CL have developed the approach of the work and have written the paper, while JFM has provided medical expertise. All authors read and approved the final manuscript.

Acknowledgements
E. Fresnel would like to thank ADIR Association for supporting her Ph.D. thesis.

Author details
[1]CORIA UMR 6614 — Normandie Université, CNRS-Université et INSA de Rouen, Campus Universitaire du Madrillet, F-76800, Saint-Etienne du Rouvray, France. [2]ADIR Association, Hôpital de Bois-Guillaume, F-76031, Rouen, France. [3]GRHV EA 3830, CHU Charles Nicolle, F-76031, Rouen, France.

Received: 11 January 2016 Accepted: 19 June 2016
Published online: 13 July 2016

References

1. Tobin MJ, Jubran A, Laghi F. Patient–Ventilator Interaction. Am J Respir Crit Care Med. 2001;163:1059–63.
2. Chopin C, Chambrin MC. Essai de classification des modes actuels de ventilation mécanique en pression positive. Réanimation Urgences. 1998;7:87–99.
3. Olivieri C, Costa R, Conti G, Navalesi P. Bench studies evaluating devices for non-invasive ventilation: critical analysis and future perspectives. Intensive Care Med. 2012;38:160–7.
4. Fauroux B, Leroux K, Desmarais G, Isabey D, Clément A, Lofaso F, Louis B. Performance of ventilators for noninvasive positive-pressure ventilation in children. Eur Respir J. 2008;31:1300–7.
5. Thille A, Lyazidi A, Richard J-C, Galia F, Brochard L. A bench study of intensive-care-unit ventilators: new versus old and turbine-based versus compressed gas-based ventilators. Intensive Care Med. 2009;35:1368–76.
6. Ouanes I, Lyazidi A, Danin PE, Rana N, Di Bari A, Abroug F, Louis B, Brochard L. Mechanical influences on fluid leakage past the tracheal tube cuff in a benchtop model. Intensive Care Med. 2011;37:695–700.
7. Lyazidi A, Thille AW, Carteaux G, Galia F, Brochard L, Richard J-C. Bench test evaluation of volume delivered by modern ICU ventilators during volume-controlled ventilation. Intensive Care Med. 2010;36:2074–80.
8. Thille AW, Rodriguez P, Cabello B, Lelouche F, Brochard L. Patient-ventilator asynchrony during assisted mechanical ventilation. Intensive Care Med. 2006;32:1515–22.
9. Nava S, Bruschi C, Rubini F, Palo A, Iotti G, Braschi A. Respiratory response and inspiratory effort during pressure support ventilation in COPD patients. Intensive Care Med. 1995;21:871–9.
10. Battisti A, Tassaux D, Janssens J-P, Michotte J-B, Jaber S, Jolliet P. Performance characteristics of 10 home mechanical ventilators in pressure-support mode: A comparative bench study. Chest. 2005;127:1784–92.
11. Richard J-C, Carlucci A, Breton L, Langlais N, Jaber S, Maggiore S, Fougère S, Harf A, Brochard L. Bench testing of pressure support ventilation with three different generations of ventilators. Intensive Care Med. 2002;28:1049–57.
12. Murata S, Yokoyama K, Sakamoto Y, Yamashita K, Oto J, Imanaka H, Nishimura M. Effects of inspiratory rise time on triggering work load during pressure-support ventilation: a lung model study. Respir Care. 2010;55:878–84.
13. Fresnel E, Muir J-F, Letellier C. Realistic human muscle pressure for driving a mechanical lung. EPJ Nonlinear Biomed Phys. 2014;2(7):. doi:10.1140/epjnbp/s40366-014-0007-8.
14. Stell IM, Paul G, Lee KC, Ponte J, Moxham J. Non-invasive ventilator triggering in chronic obstructive pulmonary disease. A test lung comparison. Am J Respir Crit Care Med. 2001;164:2092–7.

15. Costa R, Navalesi P, Spinazzola G, Rossi M, Cavaliere F, Antonelli M, Proietti R, Conti G. Comparative evaluation of different helmets on patient-ventilator interaction during non-invasive ventilation. Intensive Care Med. 2008;34: 1102–8.
16. Ferreira JC, Chipman DW, Kacmarek RM. Trigger performance of mid-level ICU mechanical ventilators during assisted ventilation: a bench study. Intensive Care Med. 2008;34:1669–75.
17. Borel JC, Sabil A, Janssens JP, Couteau M, Boulon L, Lévy P, Pépin JL. Intentional leaks in industrial masks have a significant impact on efficacy of bilevel non-invasive ventilation: a bench test study. Chest. 2009;135:669–77.
18. Ferreira JC, Chipman DW, Hill NS, Kacmarek RM. Bilevel vs ICU ventilators providing non-invasive ventilation: effect of system leaks: a COPD lung model comparison. Chest. 2009;136:448–56.
19. Costa R, Navalesi P, Spinazzola G, Ferrone G, Pellegrini A, Cavaliere F, Proietti R, Antonelli M, Conti G. Influence of ventilator settings on patient-ventilator synchrony during pressure support ventilation with different interfaces. Intensive Care Med. 2010;36:1363–70.
20. Chatburn RL. Which ventilators and modes can be used to deliver noninvasive ventilation? Respiratory Care. 2009;54(1):85–101.
21. Scott GC, Burki NK. The relationship of resting ventilation to mouth occlusion pressure. An index of resting respiratory function. Chest. 1990;98(4):900–6.
22. Budweiser S, Jörres RA, Criée C-P, Langer V, Heinemann F, Hitzl AP, Schmidbauer K, Windisch W, Pfeifer M. Prognostic value of mouth occlusion pressure in patients with chronic ventilatory failure. Respir Med. 2007;101: 2343–51.
23. Herrera M, Blasco J, Venegas J, Barba R, Doblas A, Marquez E. Mouth occlusion pressure (P0.1) in acute respiratory failure. Intensive Care Med. 1985;11:134–9.
24. Perrigault P-FO, Pouzeratte YH, Jaber S, Capdevila XJ, Hayot M, Boccara G, Ramonatxo M, Colson P. Changes in occlusion pressure (P0.1) and breathing pattern during pressure support ventilation. Thorax. 1999;54:119–23.
25. Janssens J-P, Derivaz S, Breitenstein E, De Muralt B, Fitting J-W, Chevrolet J-C, Rochat T. Changing patterns in long-term noninvasive ventilation: A 7-year prospective study in the Geneva lake area. Chest. 2003;123:67–79.
26. Brochard L. Pressure Support Ventilation. Update Intensive Care Emerg Med. 1991;15:381–91.
27. Bounoiare D. Vers une évaluation objective de l'assistance ventilatoire non invasive : synchronisabilité des ventilateurs et qualité du sommeil. Thèse de l'Université de Rouen, 2012. http://theses.fr/s149631.
28. Tassaux D, Gainnier M, Battisti A, Jolliet P. Impact of expiratory trigger setting on delayed cycling and inspiratory muscle workload. Am J Respir Critical Care Med. 2005;172:1283–9.
29. Chao DC, Scheinhorn DJ, Stearn-Hassenpflug M. Patient-ventilator trigger asynchrony in prolonged mechanical ventilation. Chest. 1997;112:1592–9.
30. Leung P, Jubran A, Tobin MJ. Comparison of assisted ventilator modes on triggering, patient effort, and dyspnea. Am J Respir Critical Care Med. 1997;155:1940–8.
31. Baydur A, Milic-Emili J. Expiratory flow limitation during spontaneous breathing: Comparison of patients with restrictive and obstructive respiratory disorders. Chest. 1997;112:1017–23.
32. Scala R, Naldi M. Ventilators for noninvasive ventilation to treat acute respiratory failure. Respiratory Care. 2008;53: 1054–80.
33. Jolliet P, Tassaux D. Clinical review: patient-ventilator interaction in chronic obstructive pulmonary disease. Critical Care. 2006;10:236.